# Combining Gaussian Fields and Fibre Processes for Modelling of Sequence Stratigraphic Bounding Surfaces

Anne-Lise Hektoen[1] Lars Holden[1] Øivind Skare[1]
Alister MacDonald[2]

[1]Norwegian Computing Center, P.O.Box 114, Blindern, N-0314 Oslo, Norway
[2]Statoil a.s., Postuttak, 7004 Trondheim, Norway

In proceedings from the 4th European Conference on the Mathematics of Oil Recovery, Røros, Norway, 7-10 June 1994

**Abstract**

The application of sequence stratigraphy concepts to reservoir description involves the correlation of different types of (bounding) surfaces from well to well to produce a high resolution reservoir zonation. A stochastic model has been developed for describing the geometry of different types of surfaces, and a reservoir zonation is constructed by simulating a number of surfaces from the base of the reservoir upwards. The surfaces are modelled as transformed Gaussian random fields. Conditioning on observed depths is performed by kriging, including inequality constraints for surfaces not observed in a well due to subsequent erosion.

This paper focusses on the stochastic model for a particular type of surface containing erosional valleys. The valleys are modelled by fibre processes and correlated Gaussian random functions. Prior distributions for valley location and geometry are defined and updated to posterior distributions by simulating from the prior model conditioned on the observations. Information such as the depth of the boundaries observed in the wells, and the well pattern with respect to valley orientation, width and sinuosity, is thus utilized in the parameter inference.

## 1 Introduction

In recent years a geological interpretation methodology known as sequence stratigraphy has become increasingly applied to subsurface reservoir description (e.g. Wagoner Van, Mitchum, Campion & Rahmanian (1990)). The

methodology places emphasis on the correlation of surfaces from well to well to provide a high resolution reservoir zonation. It differs from traditional methodologies which focus on the correlation of similar lithologies between wells. Where the geometry of the zonal bounding surfaces is associated with significant uncertainty a stochastic modelling approach is required to provide a correct basis for field development decisions.

A stochastic model has been developed for describing two types of sequence stratigraphic bounding surfaces; (1) erosional surfaces with valleys which are termed **sequence boundaries** and which are the result of a sea-level fall during the deposition of the reservoir, and (2) relatively flat surfaces termed **flooding surfaces** which are the result of a rapid sea-level rise (transgression). The framework for a reservoir model is built up by sequential simulation of the different surfaces from the base of the reservoir upwards. The surfaces define the reservoir stratigraphy. Facies and petrophysical modelling is then carried out within each stratigraphic unit.

The focus of this paper is the stochastic model for the erosive surfaces with valleys (sequence boundaries). Such surfaces are typically complex and their geometries between wells are generally associated with significant uncertainty. In fluvial reservoirs the geometry of sequence boundaries is an important variable as it controls the lateral extent of shale barriers in high net/gross intervals and the spatial distribution of reservoir sandstone in low net/gross intervals.

# 2 Sequence Stratigraphic Model

The framework for a reservoir formation is assumed to consist of several sequence stratigraphic boundaries $b_i(\mathbf{x})$ as illustrated in Figure 1. The boundaries are modelled and simulated independently starting with the deepest and then building up the reservoir by sequential transgression and erosion. Two types of bounding surfaces are modelled:

**Flooding surfaces** which form due to sea-level rise or transgression. A flooding surface is modelled as a transformed Gaussian field characterized by its expectation and covariance function. The field describes the depth within the reservoir of a flooding surface, which is typically smooth and with relatively little variability. The field can be modelled with a constant expected depth or with a linear trend in the expected depth.

**Sequence boundaries** are complex erosional surfaces which form due to sea level fall. In fluvial environments sequence boundaries are characterized by relatively flat areas termed **interfluves** and deeply eroded **incised valleys**. Two transformed Gaussian fields, characterized by their expectations and covariance functions, are used to model a single sequence boundary. The interfluve areas are modelled in a similar manner to the flooding surfaces and are defined by a transformed Gaussian field with

a constant expected depth or with a linear trend in the expected depth. The incised valleys are described by a second field describing the depth of erosion. The expectation of this field is a simulated trend surface with local valleys. The modelling and simulation of this trend surface is the focus of this paper.

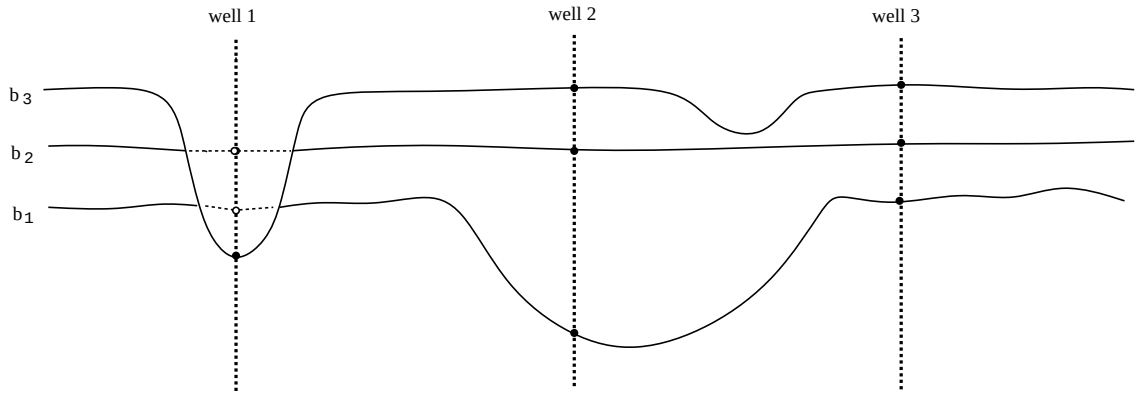


Figure 1: Cross-sectional ($x$-$z$ plane) sketch of model for sequence stratigraphic bounding surfaces where $b_1$ and $b_3$ are sequence boundaries and $b_2$ is a flooding surface. The dashed lines in bounding surface $b_1$ and $b_2$ indicate that the surfaces are eroded by bounding surface $b_3$. Observed conditioning points for the surfaces are marked with a $\bullet$, drawn conditioning points with a $\circ$.

Unconditional simulation of fields with zero expectation and specified covariance functions are performed using the screening sequential algorithm (Omre, Sølna & Tjelmeland 1993). Several different covariance functions can be used to model fields with different physical characteristics. Different anisotropies in the covariance may also be modelled.

The model is conditioned on observed boundaries in the wells. If a boundary is not observed in a well due to erosion at a later stage, it is conditioned on an observation drawn from the conditional distribution (Mardia, Kent & Bibby 1979) with the constraint that it must have a depth less than the observed sequence boundary (Figure 1). This is performed using rejection sampling. Conditioning of the simulated fields is performed by simple kriging (Journel & Huijbregts 1978). As simple kriging is used, trends in the fields are removed from the observations before conditioning and added to the field afterwards.

# 3 Modelling and simulation of trend surfaces with incised valleys

The trend surface is modelled using statistical methods similar to those developed for modelling the geometry of fluvial channel sandstones, where the sandstones are modelled as 3D objects with rectangular cross-sections (Georgsen

& Omre 1993, Georgsen, Egeland, Knarud & Omre 1994). The modelling of incised valleys involves a 2D problem (a surface instead of an object) with a more complex cross-sectional form.

The trend surface is assumed to consist of a certain number of valleys giving the depth of a 2D surface. The valleys are modelled independently and emphasis is put on finding the posterior model parameters. Data extracted from analogues (e.g. outcrops or densely drilled fields) where geometries are known, and general geological knowledge concerning the genesis of sequence boundaries and incised valleys provides the basis for a prior model, while reservoir specific observations are used to generate a posterior model which is used in the simulation.

The different stages in the modelling of the incised valleys are outlined below.

## 3.1 Model for correlation of valleys

The first step in the modelling is to define the correlation of valleys between wells. Geological interpretation is used to define the probability that a valley observed in one well lies within the same valley observed in adjacent wells.

In each simulation from the model, the actual correlations are drawn according to the specified probabilities. If no well-to-well correlation is specified the observations are assumed to be from different valleys.

## 3.2 Prior model for valley geometry

The simulation area is assumed to be rectangular in the $(x, y)$-system, where the $x$- direction is identified as the most probable direction for a valley. Each of the valleys has a principal direction given by a line. For valley number $i$, the principal direction is given by $l_s^i$. This line is parameterized by $l_s^i = \{(x, y)|(x, y) = (x_c, \theta_1^i) + s \cdot (1, \theta_2^i)\}$, with $s \in (-\infty, \infty)$ as the argument along the line; and $x_c$ being the midpoint of the reservoir-box in the $x$-direction. $l_s^i$ is fully specified by the parameter-vector $\vec{\theta^i} = (\theta_1^i, \theta_2^i)$, with $\theta_1^i$ being the $y$-coordinate of the intersection point between $l_s^i$ and the line $x = x_c$; and $\theta_2^i$ being the slope of $l_s^i$. (Figure 2).

Consider an arbitrary valley $i$, and let everything related to it be referenced by $s$ along the principal direction $l_s^i$. Then the position and shape of the valley, at reference $s$, is defined by a multi-dimensional vector:

$$(1) \quad \vec{V}^i(s) = \{U_{DL}^i(s), U^i(s)\} = \{U_{DL}^i(s), U_D^i(s), U_W^i(s), U_T^i(s), U_{DP}^i(s)\},$$

with $U_{DL}^i(s)$ being low frequency deviation of the center line from the principal direction line of valley $i$; $U_D^i(s)$ a higher frequency deviation of the center line from $U_{DL}^i(s)$; $U_W^i(s)$ being the width; $U_T^i(s)$ being the maximum depth, and $U_{DP}^i(s)$ being the deepest point of valley $i$ relative to the valley centerline $U_{DL}^i(s) + U_D^i(s)$ (i.e. an asymmetry term).

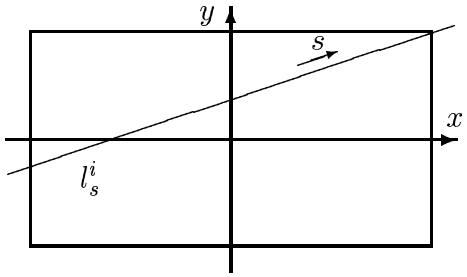


Figure 2: Direction line for one valley, intersecting the area of interest.

A cross-section of a valley is assumed to have the shape of two polynomials of the form $c_0 \cdot r^\rho + c_1$ where $r$ is measured normal to the line, with $r = 0$ in the position of the deepest point. $c_0$ and $c_1$ are constants which can be computed from the vector $U^i(s)$, see Figure 3, and $\rho$ a shape-parameter specifying the cross-sectional form of the valley as shown in Figure 4. High $\rho$ values lead to the simulation of steep valley margins, whereas low values result in more gently dipping valley sides.

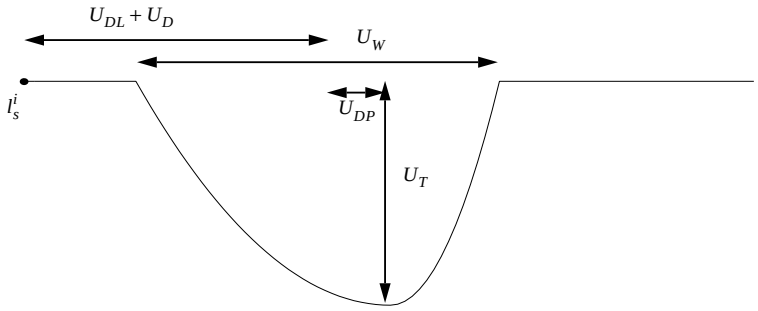


Figure 3: Cross-section of the reservoir perpendicular to the principal direction of the valley.

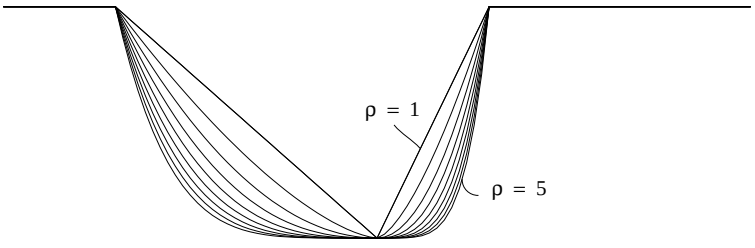


Figure 4: Cross-section of the reservoir perpendicular to the principal direction of the valley showing cross-sectional forms of a valley generated with $\rho \in (1, 5)$.

$U^i_{DL}(s)$ is uncorrelated with the vector $\vec{U}^i(\cdot)$ and is defined as a 1-dimensional

Gaussian function with properties given by:

$$(2) \qquad \mathrm{E}\{U_{DL}(s)\} = 0 \quad \mathrm{Cov}\{U_{DL}(s), U_{DL}(s')\} = \sigma^2_{DL}\rho_{DL}(|s-s'|)$$

where $\sigma^2_{DL}$ is the variance and $\rho_{DL}(\cdot)$ is the spatial correlation-function.

The vector $\vec{U}^i(\cdot)$ is defined as a 4-dimensional correlated Gaussian function, with reference along $l^i_s$. The univariate properties of this function, are given by:

$$(3) \quad \begin{array}{llll} \mathrm{E}\{U_D(s)\} & = 0 & \mathrm{Cov}\{U_D(s), U_D(s')\} & = \sigma^2_D\rho_D(|s-s'|) \\ \mathrm{E}\{U_W(s)\} & = \mu_W & \mathrm{Cov}\{U_W(s), U_W(s')\} & = \sigma^2_W\rho_W(|s-s'|) \\ \mathrm{E}\{U_T(s)\} & = \mu_T & \mathrm{Cov}\{U_T(s), U_T(s')\} & = \sigma^2_T\rho_T(|s-s'|) \\ \mathrm{E}\{U_{DP}(s)\} & = \mu_{DP} & \mathrm{Cov}\{U_{DP}(s), U_{DP}(s')\} & = \sigma^2_{DP}\rho_{DP}(|s-s'|), \end{array}$$

where the parameters $\mu_W$, $\mu_T$ and $\mu_{DP}$ are the expected width, thickness and deepest point (relative to centerline) of the valleys, $\sigma^2_\cdot$ the variance, and $\rho_\cdot(\cdot)$ the spatial correlation-function. Gaussian correlation functions are used, resulting in smooth fields. As the magnitudes of the univariate properties cannot be estimated precisely using analogue data and geological knowledge, it is generally advisable to specify prior distributions for all the parameters in order to capture the true uncertainty associated with the modelling.

Correlation between the variables may be included in the model. With pointwise correlation between two variables $\alpha, \beta \in \{D, W, T, DP\}$ given by $\rho_{\alpha\beta}$, the spatial correlation is defined as:

$$(4) \qquad \mathrm{Cov}\{U_\alpha(s), U_\beta(s')\} = \sigma^2_{\alpha\beta} \cdot \rho(|s-s'|)$$

where $\sigma^2_{\alpha\beta} = \sigma_\alpha\sigma_\beta\rho_{\alpha\beta}$, and $\rho(\cdot) = \rho_\alpha(\cdot) = \rho_\beta(\cdot)$ for **correlated** variables.

It is straightforward to simulate valleys from the prior model when there are no observations. The following sections is therefore devoted to the difficult problem of generating valleys from a posterior distribution conditioned on well data.

## 3.3 Posterior model for valley geometry

In addition to the prior model, observations from wells provide reservoir specific information which should be utilized for estimation of model parameters. In the model for incised valleys, depth of boundaries in the wells and the well pattern with respect to valley orientation, width and sinuosity is utilized. Realizations are generated from a posterior model taking this information into account.

The shape of a valley cross-section makes the conditioning highly nonlinear. The position of a well observation within a valley cross-section is not known and an observation therefore only provides a lower limit for the maximum valley depth ($U_T$). A small measured depth value may either indicate that the

valley is shallow or that the well is located far from the center of the valley. Irregular well spacing makes the posterior distribution complicated to find analytically, hence the posterior distribution is found implicitly by simulating from the prior model conditioned on the observations.

**Finding posterior model, direction line and conditioning points** As each valley is modelled as a multidimensional Gaussian field, it is possible to combine any principal direction, expected depth, width, etc. with well observations and still have a positive probability. The simulation algorithm used to find the posterior model parameters, direction line and conditioning points for the correlated Gaussian fields is therefore based on repeated drawing from the prior distribution with conditioning.

For each valley, $N$ lines with corresponding model parameters and conditioning points are simulated according to the following algorithm.

1. For $j = 1..N$ {
   (a) Find the expectation, standard deviation and range for the vector $V = (U_{DL}, U_D, U_W, U_T, U_{DP})$ and the valley-shape $\rho$ by drawing from the specified prior distributions.
   (b) Draw a line $l_j$ from the prior distribution which is inside the area of interest.
   (c) Find conditioning point $U^i_{DL}$ in each well position $s_i$ given the line $l_j$ by sequential simulation.
   (d) Find a set of conditioning points $U^i = (U^i_D, U^i_W, U^i_T, U^i_{DP})$ in each well position $s_i$, given the line $l_j$ and $U^i_{DL}$, by sequential simulation. The first vector $U_1$ is drawn from the prior distribution, while vector $U_i$, $i = 2\ldots$ is drawn from the distribution conditioned on previous simulated vectors. An approximation is made by only conditioning on vector $U_{i-1}$.
      - If a valley thickness is observed in the actual well position draw $M$ different vectors $U^i$ describing the valley cross section in the plane normal to the line, and interpolate the 2 closest vectors to get an exact match of $U^i$ in the well position. A typical number of cross-sections to draw is $M = 10$.
      - If no observed valley thickness, draw a vector $U^i$ not penetrated by the well.
   (e) Calculate the 'probability' of line $l_j$ from the multi normal probability density function.
   }
2. Draw one of the lines, with a corresponding set of model parameters and conditioning points, with probability proportional with the calculated probability of the line.

By using the algorithm described above sampling from the posterior distribution is achieved. Reservoir specific observations are taken into account in addition to the prior model, and the simulation algorithm generates realizations with principal directions relative close to the wells and with realistic expected depths.

### 3.4 Simulation of trend surface with incised valleys

Each valley in the surface is simulated independently. First valleys observed in wells are simulated, then the number of unobserved valleys are drawn from a distribution and these valleys simulated. The simulation procedure for each valley consists of two steps:

A. Simulate a line and a valley shape. If there are well observations; simulate also a set of conditioning points in each well-position, for both penetrating and not-penetrating wells. The algorithm used for conditional simulations from the posterior model was described in details above.

B. Simulate the full Gaussian functions on a discrete grid along the direction line by simulating unconditional correlated functions. If there are wells; condition on the set of points found in A. above using kriging.

As the valleys are simulated independently, the sampling space is manageable, and as a sequential approach is used in the conditional simulation the algorithm is relatively fast.

## 4 An example

The model presented above is illustrated by an example where a synthetic reservoir stratigraphy within a volume of 4000 m $\times$2000 m $\times$50 m is defined by three sequence boundaries (SB1, SB2, SB3) and three flooding surfaces (FS1, FS2, FS3). The example is conditioned on six wells. A cross-section through a realization is illustrated in Figure 5 and some of the parameter values in the prior model are listed in Table 1. The Gaussian fields describing the flooding surfaces and sequence boundaries are modelled with Gaussian covariance functions with large ranges and small variances, resulting in smooth fields.

The example is intended to illustrate the following features of the model: (1) uncertainty in correlation; (2) the number of lines to be drawn from the prior model in order to define a stable posterior model; (3) the combined influence of the prior width distribution and the well pattern on the posterior distribution of valley directions; and (4) the influence of well observations on the posterior distribution for valley depths ($U_T$).

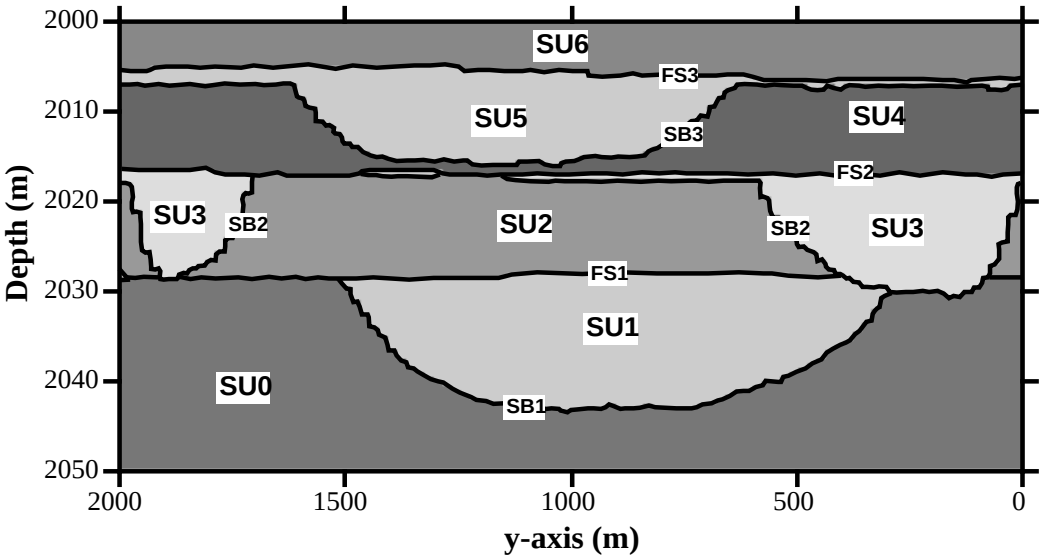


Figure 5: Cross-section through reservoir with 3 flooding surfaces and 3 sequence boundaries defining 7 stratigraphic units, SU0-SU6.

| | $(\mu_T, \sigma_T, R_T)$ | $(\mu_W, \sigma_W, R_W)$ | $\varphi$ | Well correlations |
|---|---|---|---|---|
| sb1 | $(12, 2, 3000)$ | $(1000, 200, 2000)$ | $N(0, 20)$ | $P(3,4,5) = 1$ |
| sb2 | $(14, 3, 2000)$ | $(400, 80, 800)$ | $N(30, 5)$ | $P(2,4) = 0.5$ |
| sb3 | $(N(5.5, \sigma_{\mu_T}), 0.2 \cdot \mu_T, 250 \cdot \mu_T)$ | (900,90,1350) | $N(45, 20)$ | $P(2,7) = P(5,8) = 1$ |

Table 1: Parameters in models used to generate the realizations in Figure 5-12. The models for depth $U_T$ and width $U_W$ are specified by expectations $\mu_T, \mu_W$, standard deviations $\sigma_T, \sigma_W$ and spatial correlation lengths/ranges $R_T, R_W$. The direction of the line is specified by an angle $\varphi$ relative to the $x$- direction. Well-to-well correlations are specified as e.g. $P(2,4) = 0.5$ which means that well 2 and 4 are in the same valley with probability 0.5.

**Well-to-well correlations of valleys** The first step in every simulation of a trend surface is to identify which observations to condition on within each valley. For sequence boundary 2 there is some uncertainty in the interpretation of whether well 2 and 4 are in the same valley or not, hence a probability 0.5 is specified for both wells to be in the same valley (Table 1). Figure 6 and 7 illustrate two different realizations from the same model generated using different seed numbers.

**Number of lines used to define a posterior distribution** Recall from the previous section that $N$ lines with corresponding model parameters and conditioning points are simulated in order to find the line, posterior parameters and conditioning points for one valley. The number $N$ is model dependent. For sequence boundary 1 a suitable number $N$ is found by inspecting the probability of the chosen line with increasing $N$ and the same start seed. Figure 8 shows the logarithm of the probability-density of the chosen line as

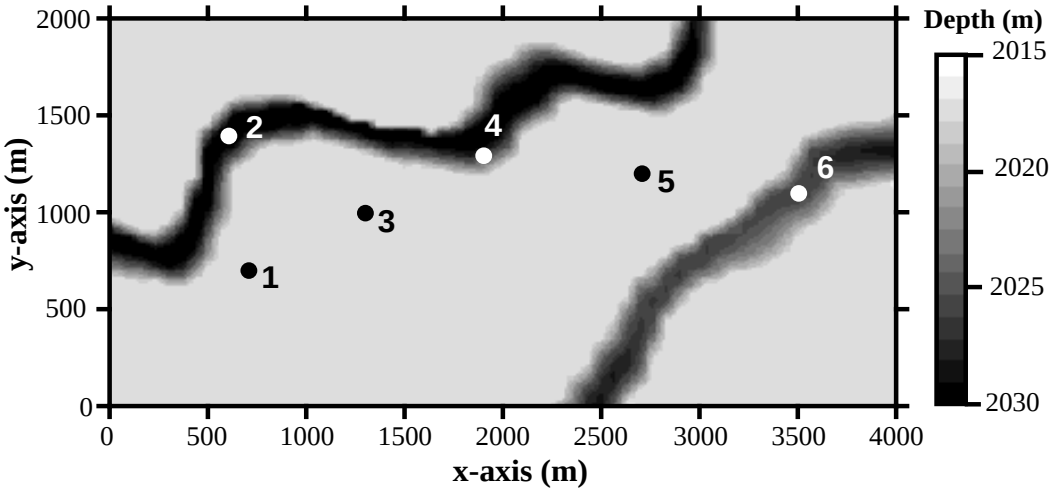


Figure 6: Realization 1 of trend surface for sequence boundary 2. Correlation of well 2 and 4 gives a realization with two valleys.

a function of $N$ for five different seed numbers. The figure shows that the probability of the chosen line increases with increasing $N$ up to a plateau for $N$ values $> 50$, i.e. the algorithm has converged with respect on the probability. Hence $N = 50$ is used in this particular example.

**Bayesian updating of line direction** Sequence boundary 1 is interpreted to consist of a single valley which is observed in three of the six wells. In the prior model the expected valley direction is parallel to the $x$-axis and with a moderate uncertainty in the angle (Table 1). The chosen direction lines for 20 different realizations are illustrated in Figure 9. The first ten have been chosen based on a prior model where the expected width of the valley is 500 m and the second ten based on a prior model where the expected width is 1500 m. Where narrow valleys are assumed, the resultant valley direction lines must be oriented approximately E-W in order to honour the prior model and well observations (Figure 9a), whereas a prior model with wider valleys changes the resultant orientation to more SE-NW and NE-SW (Figure 9b). This interdependence between parameters and between parameters and observations is an important aspect of the posterior model as such interdependencies are physically sensible, but difficult to estimate in a prior model.

**Bayesian updating of the depth distribution** Sequence boundary 3 is interpreted to comprise 2 separate valleys. The first is observed in well 2 at a depth of 2010.9 m and the second in well 5 at a depth 2014.3 m. The expected depth for the non-incised areas of the surface is 2006.8 m and the observed valleys are thus 4.1 m and 7.5 m deep at well 2 and well 5 respectively. Figure 10 illustrates a realization from a prior model with a constant value for expected valley depth of 5.5 m (i.e. the average depth to the valley axis should

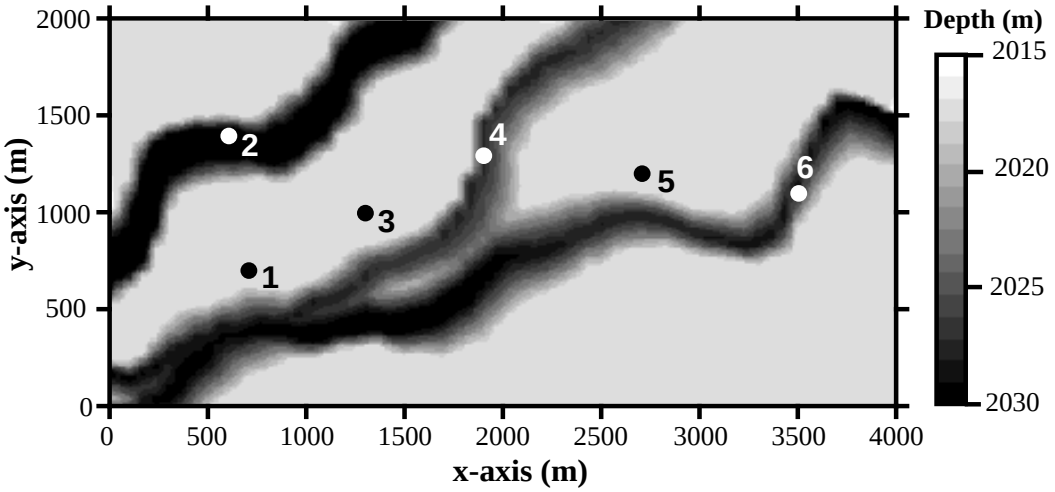


Figure 7:
Realization 2 of trend surface for sequence boundary 2. No correlation of well 2 and 4 gives a realization with 3 valleys.

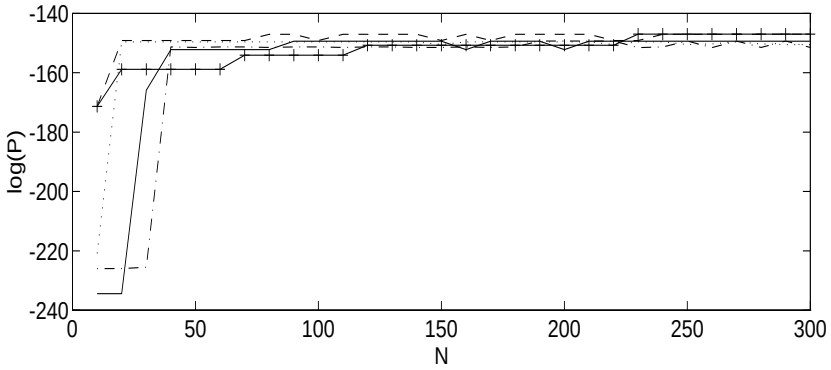


Figure 8: Logarithm of probability density as a function of number of lines $N$. 5 sequences of realizations using different start seeds are illustrated.

be 2012.3 m). Figure 11 on the other hand is based on a prior model with uncertainty in the expected valley depth. A single observation of each valley has only a moderate influence on the posterior model and in this particular example two relatively deep valleys have been generated even although the observation in well 2 allows for the generation of a shallower valley.

Two observations of the same valley have a stronger influence on the posterior model and Figure 12 illustrates a realization from the same prior model as that used for Figure 11, but with two observations of each valley. As both observations of the first valley (in wells 2 and 7) occur at rather shallow depths, it is most probable that the valley is shallow. Likewise both observations of the second valley (in wells 5 and 8) are relatively deep, and it is most probable that the second valley is deep. The resultant realization illustrates one shallow

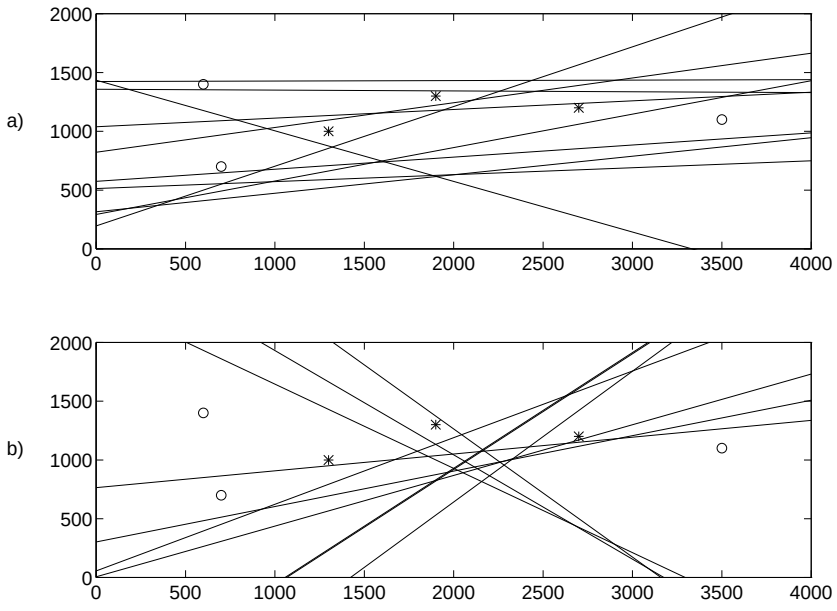


Figure 9: The chosen direction lines from 20 realizations of sequence boundary 1. a) $\mathrm{E}(U_{HW}) = 500$ m, b) $\mathrm{E}(U_{HW}) = 1500$ m. Wells within the valley are marked with a $*$, wells outside with a $\circ$.

and one deep valley simulated from the posterior model (Figure 12).

# 5 Final remarks

In response to the increasing application of sequence stratigraphy as a geological interpretation methodology, a stochastic model has been developed to describe the geometry of sequence stratigraphic bounding surfaces. Other stochastic models can easily be used to model heterogeneities such as small or large barriers, fluvial channels etc. within the stratigraphic units or along the stratigraphic bounding surfaces.

The model provides a large degree of user control, and it is possible to meet the challenge of a complex conditioning scheme including well-to-well correlation, inequality constraints and non-linear conditioning. The use of prior distributions containing significant uncertainty in the model parameters is necessary as the exact values of the parameters cannot be estimated.

We have concentrated on modelling of sequence boundaries as they, in fluvial reservoirs, control the lateral extent of shale barriers in high net/gross intervals and the spatial distribution of reservoir sandstone in low net/gross intervals. Gaussian fields have appeared to be well suited for modelling of the complex geometry in these surfaces because of the large degree of flexibility associated with the trend surfaces.

A formally correct Bayesian updating methodology with a complex conditioning scheme has been developed for simulation of the trend surfaces. The

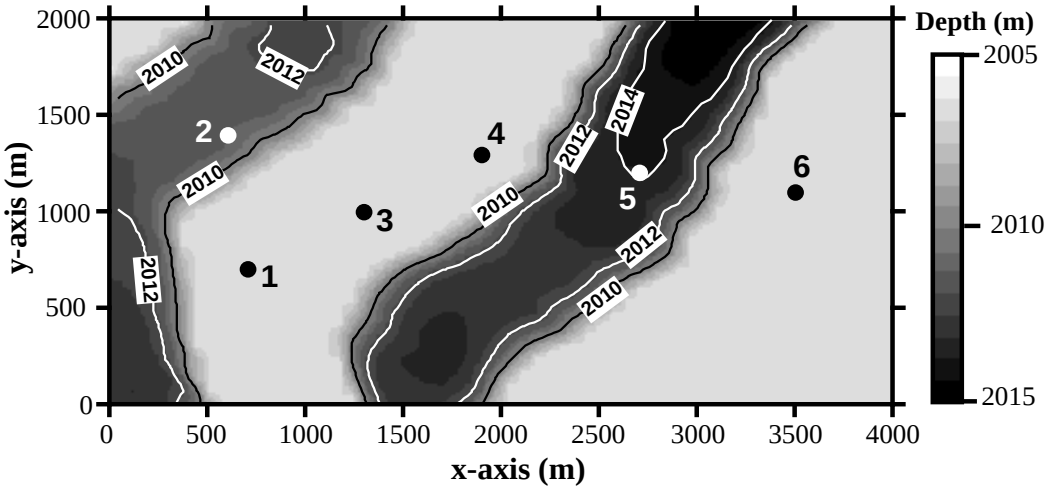


Figure 10: Realization of trend surface for sequence boundary 3. 6 wells. No uncertainty in specified prior: $\mu_T \sim N(5.5, 0)$.

method draws repeatedly from the prior distributions with conditioning on observations to produce an implicit posterior model. This method should have application to other complex parameter inference problems where it is desirable to draw on both field specific observations and general geological information.

# Acknowledgements

The research has been financed by the JOULE II Reservoir Engineering Project and Statoil a.s. The authors want to express their thanks to Statoil a.s. for permission to publish this paper.

# References

Armstrong, M. & Dowd, P., eds (1994), *Geostatistical Simulations*, Vol. 7 of *Quantitative Geology and Geostatistics*, Proceedings of the Geostatistical Simulation Workshop, Fontainebleau, France, 1993, Kluwer Academic Publishers, Dordrecht.

Georgsen, F. & Omre, H. (1993), Combining fibre processes and Gaussian random functions for modelling fluvial reservoirs, *in* Soares (1993), pp. 425–440.

Georgsen, F., Egeland, T., Knarud, R. & Omre, H. (1994), Conditional simulation of facies architecture in fluvial reservoirs, *in* Armstrong & Dowd (1994), pp. 235–250.

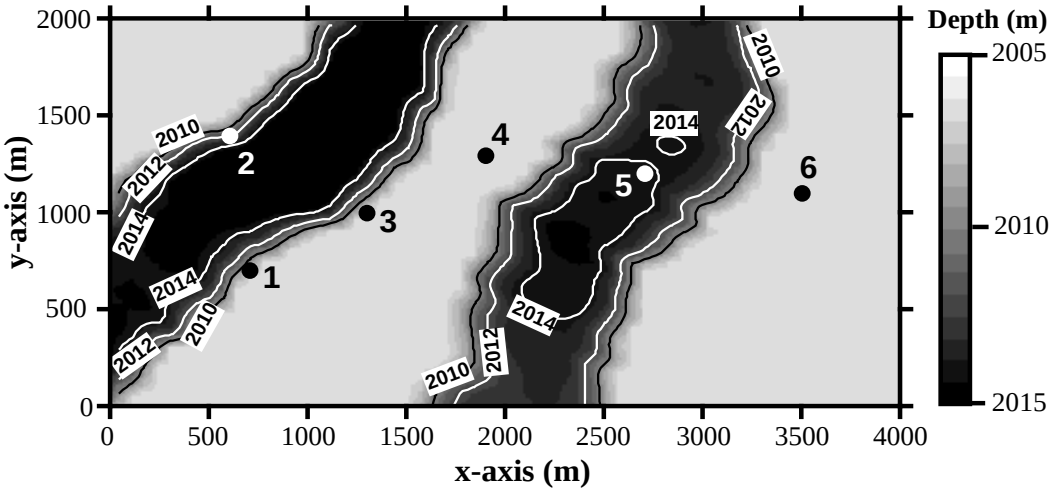


Figure 11: Realization of trend surface for sequence boundary 3. 6 wells. Specified prior: $\mu_T \sim N(5.5, 2)$. Simulated posterior values: $\mu_T = 7.36$ (left valley) and $\mu_T = 6.17$ (right valley).


Journel, A. G. & Huijbregts, C. J. (1978), *Mining Geostatistics*, Academic Press Inc., London.

Mardia, K. V., Kent, J. T. & Bibby, J. M. (1979), *Multivariate Analysis*, Academic Press Inc., London.

Omre, H., Sølna, K. & Tjelmeland, H. (1993), Simulation of random functions on large lattices, *in* Soares (1993), pp. 179–199.

Soares, A., ed. (1993), *Geostatistics Tróia '92*, Vol. 5 of *Quantitative Geology and Geostatistics*, proceedings from '4th International Geostatistics Congress', Tróia Portugal, 1992, Kluwer Academic Publishers, Dordrecht. 2 volumes.

Wagoner Van, J. C., Mitchum, R. M., Campion, K. M. & Rahmanian, V. D. (1990), *Siliciclastic Sequence Stratigraphy in Well Logs, Cores, and Outcrops: Concepts for High-Resolution Correlation of Time and Facies*, AAPG Methods in Exploration Series, No. 7, The American Association of Petroleum Geologists, Tulsa, Oklahoma 74101.

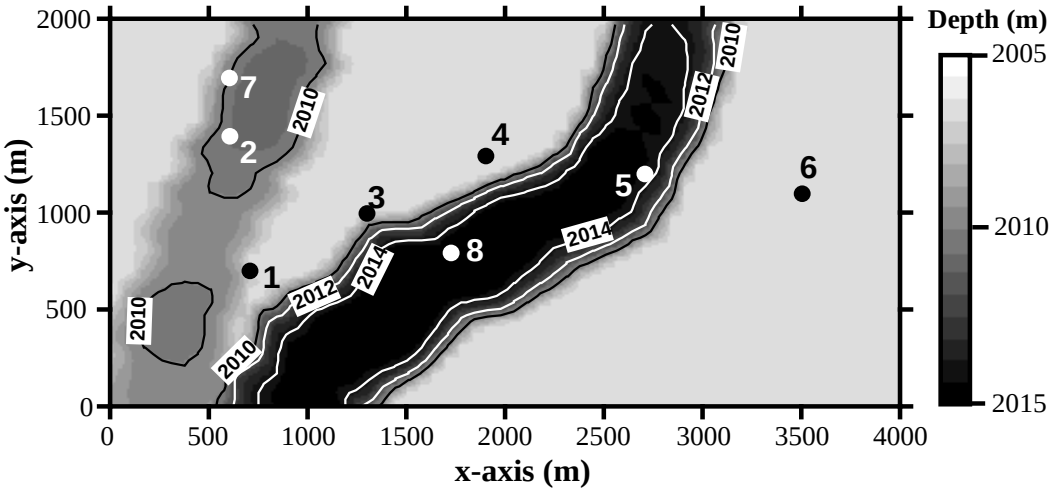


Figure 12: Realization of trend surface for sequence boundary 3. 8 wells. Specified prior: $\mu_T \sim N(5.5, 2)$. Simulated posterior values: $\mu_T = 3.58$ (left valley) and $\mu_T = 6.75$ (right valley).